Two-photon energy distribution from the decay of the 2 $^1S_0$ state in He-like uranium

D. Banaś,[1,*] A. Gumberidze,[2,3] S. Trotsenko,[4,5] A. V. Volotka,[6,7] A. Surzhykov,[4,8] H. F. Beyer,[4] F. Bosch,[4] A. Bräuning-Demian,[4] S. Fritzsche,[5,9] S. Hagmann,[4,10] C. Kozhuharov,[4] A. Kumar,[11] X. Ma,[12] R. Mann,[4] P. H. Mokler,[4] D. Sierpowski,[13] U. Spillmann,[4] S. Tashenov,[4,8] Z. Stachura,[14] A. Warczak,[13] and Th. Stöhlker[4,5,15]

[1]*Institute of Physics, Jan Kochanowski University, PL-25-406 Kielce, Poland*

[2]*ExtreMe Matter Institute EMMI and Research Division, GSI Helmholtzzentrum für Schwerionenforschung, D-64291 Darmstadt, Germany*

[3]*FIAS Frankfurt Institute for Advanced Studies, D-60438 Frankfurt am Main, Germany*

[4]*GSI Helmholtzzentrum für Schwerionenforschung, D-64291 Darmstadt, Germany*

[5]*Helmholtz-Institut Jena, D-07743 Jena, Germany*

[6]*Institut für Theoretische Physik, Technische Universität Dresden, D-01062 Dresden, Germany*

[7]*Department of Physics, St. Petersburg State University, St. Petersburg 198504, Russia*

[8]*Physikalisches Institut, Ruprecht-Karls-Universität, D-69120 Heidelberg, Germany*

[9]*Theoretisch-Physikalisches Institut, Friedrich-Schiller-Universität Jena, D-07743 Jena, Germany*

[10]*Institut für Kernphysik, Universität Frankfurt, D-60438 Frankfurt am Main, Germany*

[11]*Nuclear Physics Division, Bhabha Atomic Research Centre, Trombay, Mumbai 400085, India*

[12]*Institute of Modern Physics, Lanzhou 730000, China*

[13]*Institute of Physics, Jagiellonian University, PL-30-059 Cracow, Poland*

[14]*Institute of Nuclear Physics PAN, PL-31-342 Cracow, Poland*

[15]*Institut für Optik und Quantenelektronik, Friedrich-Schiller-Universität Jena, D-07743 Jena, Germany*

(Received 16 April 2013; published 21 June 2013)

We have performed a measurement of the spectral shape from the two-photon decay of the $1s2s\ ^1S_0$ state in He-like uranium. The two-photon emission followed the ionization of initially Li-like uranium ions in collisions with a N_2 gas-jet target. The measured shape of the two-photon energy distribution shows good agreement with results of the relativistic calculations that take into account the electron-electron interaction rigorously up to the first order in quantum electrodynamic perturbation expansion. From the full width at half maximum of the measured two-photon energy distribution, we confirm the theoretically predicted modification of the shape due to the relativistic effects.

DOI: 10.1103/PhysRevA.87.062510 PACS number(s): 32.30.Rj, 31.30.jc, 32.80.Wr

I. INTRODUCTION

Highly charged heavy ions are specific atomic systems where relativistic and quantum electrodynamic (QED) effects play a significantly enhanced role compared to neutral (light) atoms. In these systems, very strong Coulomb fields produced by the heavy nuclei and a reduced electron screening, rapidly increase the importance of inner shell radiative processes and especially the probabilities of otherwise forbidden transitions. In particular, since the decay rates of allowed $E1$ transitions scale with the nuclear charge (Z) approximately as Z^4, while for various forbidden transitions ($M1$, $M2$, $E2$, $2E1$, and spin-forbidden $E1$) as Z^6–Z^{10}, the latter become especially important in highly charged high-Z ions.

Besides studies and spectroscopy of single-photon transitions, two-photon decays in heavy ions have also attracted much experimental and theoretical attention. These transitions occur via simultaneous emission of two correlated photons and are fundamental examples of second-order atomic processes. From the viewpoint of atomic theory, the analysis of these two-photon transitions requires detailed knowledge of the entire level structure of an ion (or an atom), and hence, it enables one to study relativistic, many-body and even QED effects in heavy atomic systems. The two-photon transitions are especially important for the cases where a single-photon decay is strictly forbidden by the angular momentum conservation, e.g., between the levels with the total angular momentum $J_i = J_f = 0$. Göppert-Mayer was the first to suggest the existence of two-photon transitions [1]. They were further studied in the classic paper of Breit and Teller [2]. Since then, numerous experimental studies of the two-photon transitions in H-like and He-like ions have been performed [3]. Most of them are based on lifetime measurements of the states emitting the two photons, namely, the $2s_{1/2}$ state in H-like and $1s2s\ ^1S_0$ (shortly denoted as $2\ ^1S_0$), $1s2s\ ^3S_1$ ($2\ ^3S_1$), and $1s2p\ ^3P_0$ ($2\ ^3P_0$) states of He-like ions. For the latter, the first measurements of the lifetimes have been performed by Pearl [4] and van Dyck *et al.* [5] for helium, Prior and Shugart [6] for Li^+ ions, and by Marrus and Schmieder [7] for Ar^{16+} ions. During the following years, measurements of the lifetimes of the $2S$ levels in He-like ions were performed for Ni^{26+} and Br^{33+} ions by Dunford *et al.* [8–12], for Kr^{34+} and Xe^{52+} ions by Marrus *et al.* [13,14], and for Nb^{39+} ions by Simonovici *et al.* [15]. In addition, measurements of the lifetime of the metastable $2\ ^3P_0$ state in He-like gold and uranium were carried out by Toleikis *et al.* [16] and Munger and Gould [17].

In spite of the high precision in measuring the lifetimes of the two-photon transitions, such experiments can only test the total (two-photon) decay probabilities summed over all the continuum photon energies and become very difficult for high-Z systems where the lifetimes of the levels are very short. More detailed information about the influence of relativistic and many-body effects on the two-photon transitions can be

*d.banas@ujk.edu.pl

delivered by measurements of the spectral distribution of the emitted photons. The first observations of the spectral shape of the two-photon decays were made by Lipeles *et al.* [18] for He^+, by Elton *et al.* [19] for He-like Ne IX ions, and by O'Connell *et al.* [20] for metastable atomic hydrogen. For He-like heavy ions, the spectral distribution of the two-photon decay from the $2\,^1S_0$ state was studied by Ali *et al.* [21,22] for Kr^{34+} and followed by measurements for Ni^{26+} ions by Schäffer *et al.* [23] and Dunford *et al.* [24], and for Au^{77+} by Schäffer *et al.* [25]. Here, we would like to note that the $2\,^1S_0 \rightarrow 1\,^1S_0$ two-photon decay is dominated by the electric dipole ($2E1$) channel, while the higher-multipole contributions are negligible for the total rates and energy distributions. Recently, an experimental approach has been developed in our group and successfully applied for measuring the $2E1$ transition spectral shape in He-like tin [26]. All these experiments have shown that study of the two-photon energy distribution is a very sensitive probe for testing of state-of-the-art atomic structure theories. Moreover, they stressed the importance of using heavy ions for detailed studies of the relativistic effects which, as expected, become more prominent in the high-Z domain.

From the theoretical side, the first accurate nonrelativistic calculations of the two-photon decay rates for the $2\,^1S_0$ state in He-like ions with nuclear charges Z from 2 to 92 were performed by Drake [27] who also estimated the relativistic corrections to the rates. He showed that the nonrelativistic two-photon decay rates increase continuously with Z, while the rates taking into account the relativistic corrections show a maximum around $Z = 42$ and then decrease gradually for higher Z [27]. Note that, for this comparison, both rates were normalized to Z^6. First fully relativistic calculations of the $2E1$ decay rates and photon energy distributions for the $2\,^1S_0$ state in He-like ions with nuclear charges Z from 2 to 100 were carried out within the configuration-interaction method by Derevianko and Johnson [28]. Their calculations showed that the nonrelativistic approach overestimates the rates by about 30% for high Z. The evaluated relativistic effects leading to the reduction of the normalized decay rates for high-Z ions appear to be in excellent agreement with the earlier estimation by Drake [27]. Derevianko and Johnson also studied the Z dependence of the spectral distribution and found that the reduced width of the energy distribution changes considerably as a function of Z due to an interplay between the electron-electron correlation and the relativistic effects [28].

Recently, the two-photon decay rates and spectral distributions have been evaluated within the QED framework for the $2\,^1S_0 \rightarrow 1\,^1S_0$ and $2\,^3S_1 \rightarrow 1\,^1S_0$ transitions [29]. This calculation takes into account the electron-electron interaction rigorously up to the first order in the QED perturbation expansion. In contrast to [28], where for treatment of the electron-electron interaction the Breit approximation was employed, the QED approach allows one to use the full photon propagator, i.e., without an expansion in αZ (where α is the fine-structure constant). The values for the $2\,^1S_0$ decay rates obtained in [29] deviate slightly from those of Ref. [28], and the difference grows with increasing Z. The calculations of [29] also confirm the large relativistic effects on the spectral distribution of the two-photon decay of the $2\,^1S_0$ state.

In this paper, we report on a measurement of the $2E1$ two-photon energy distribution from the decay of the $1s2s\,^1S_0$ level in He-like uranium. For the measurement, we utilized a recently developed experimental technique [26,30]. The paper is organized as follows: In Sec. II the experimental arrangement is presented, the measurement method and its consequences on the measured x-ray spectra are shown in Sec. III, the analysis of the experimental spectra is presented in Sec. IV, and the obtained results together with the theoretical predictions are discussed in Sec. V. Finally, a summary and outlook are given in Sec. VI.

II. EXPERIMENT

The measurement was performed at the experimental storage ring (ESR) at GSI in Darmstadt. For the experiment, an intense beam of lithium-like uranium ions with an initial energy of 398 MeV/u was delivered by the UNILAC/SIS complex. In order to obtain the intense Li-like uranium beam at the beam energies needed for the present experiment, a carbon stripper foil with a thickness of 10 mg/cm^2 (a thickness much below the equilibrium thickness) was mounted in the beam transfer line between the synchrotron (SIS) and the ESR. In contrast to the commonly used copper strippers in the SIS/ESR transfer channel, such carbon foils provide a high yield of heavy multielectron ions [31].

The Li-like uranium ions were accumulated in the ESR and cooled by the electron cooler with a 200 mA electron beam. The accumulated ions, forming a beam with a FWHM of $\sim$2 mm were colliding with a supersonic N_2 gas-jet target with a typical areal density of $\sim 10^{12}$ atoms/cm^2. The beam energy loss, due to the interaction with the target, was compensated by the continuous electron cooling.

A scheme of the experimental setup is shown in Fig. 1. The x rays produced in collisions of the ions with the target were registered by an array of germanium detectors mounted at different observation angles with respect to the ion beam direction. The detectors placed at 35°, 90°, and 150° were separated from the ultrahigh vacuum system of the interaction chamber by 100 μm beryllium windows, whereas the detectors placed at 60° and 120° were separated by 50-μm steel windows. At the observation angle close to 0° a segmented

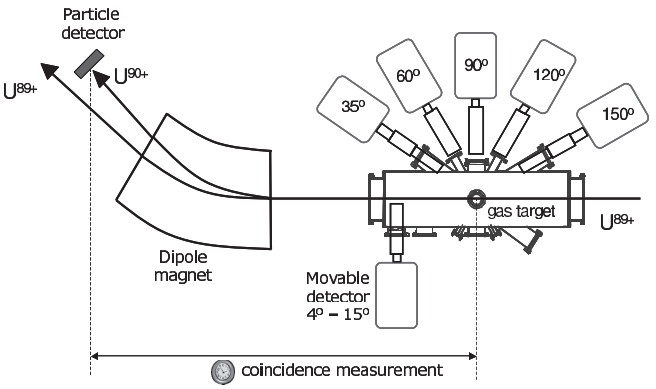

FIG. 1. A scheme of the experimental setup at the ESR storage ring showing the interaction chamber, x-ray detectors arrangement, dipole magnet, and the particle detector position.

germanium detector consisting of four individual strips was mounted. The detector was protected from the high-energy electron background by a 1-mm aluminum absorber. In front of all the detectors vertical slits made out of copper and lead assembly with 6-mm openings were mounted in order to confine the angular acceptance, thus reducing the Doppler broadening. A typical energy resolution of the detectors used was in the range of 500–600 eV at 120 keV photon energy. The projectile ions that lost one electron due to the interaction with the target were separated from the beam in the ESR dipole magnet downstream from the target chamber and registered by a multiwire proportional counter placed after the magnet. The x rays were recorded in a (so-called) single mode in which no hardware coincidence condition was applied. Instead, every x-ray photon was first accepted as a trigger to read out the energy and time information from all the detectors provided by analog-to-digital converter and time-to-digital converter modules. In this way, the coincidence information between the emitted x rays and the ions which have lost one electron was also acquired. For the data accumulation, a beam time of $\sim$120 h was used.

The detectors were calibrated using radioactive sources of ^{57}Co, ^{133}Ba, ^{152}Eu, ^{207}Bi, and ^{241}Am. Special attention was paid to the accurate determination of the detector efficiencies close to the Ge-K absorption edge (11.2 keV), which was important for the observation angles larger than 90°, for which the detected photon energies were relatively low because of the Doppler shift. The detector efficiencies were analyzed using a procedure suggested by Pajek *et al.* [32] for Si(Li) detectors and here extended to germanium detectors. The fitting of the efficiency curves was performed for the energy range from the Ge-K absorption edge up to the 1770 keV γ line of ^{207}Bi, resulting in overall efficiency uncertainties of $\sim$3%.

III. SELECTIVE K-SHELL IONIZATION

In the experiment, Li-like uranium ions in the $1s^2 2s$ ground state moving with an energy of 398 MeV/u were colliding with a N_2 gas-jet target. In these collisions, excited He-like uranium ions can be formed by a K-shell ionization of the initially Li-like system (L-shell ionization does not produce excited He-like ions). Utilizing the coincidence time information provided by our data acquisition system (see Sec. II), we observed the x-ray spectra emitted during the decay of the produced excited He-like ions. As an example, a spectrum registered in coincidence with the up-charged (ionized) uranium ions by the Ge(i) detector placed at 35° is shown in Fig. 2. Only two features are observed in the measured spectra: a broad continuum, which can be identified as a result of the two-photon $2E1$ decay of the $2\,^1S_0$ state and an intense monoenergetic line from the magnetic dipole $M1$ transition of the $2\,^3S_1$ level (see the level scheme shown in Fig. 3). For both of these states, i.e., $2\,^1S_0$ and $2\,^3S_1$, electric dipole transitions ($E1$) to the ground state are strictly forbidden by selection rules. No additional lines from decays of the $2\,^1P_1$ ($E1$ dipole transition) and $2\,^3P_2$ ($M2$ magnetic quadruple transition) states are observed. This means that in the collision leading to the K-shell ionization of the Li-like ions, the probability of a simultaneous $2s$ electron excitation is very small and thus the $2s$ electron remains almost unaffected.

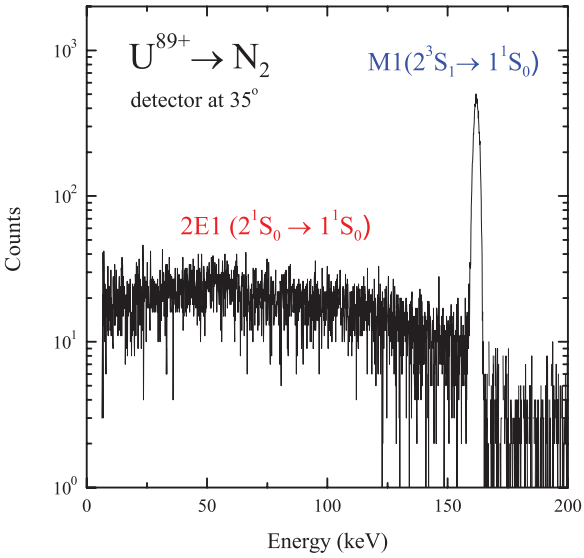

FIG. 2. (Color online) X-ray spectrum registered by the detector placed at an observation angle of 35°, measured in coincidence with the ionization of initially Li-like ions. In the spectrum, only two transitions can be identified: the $M1$ transition from the decay of the $2\,^3S_1$ level and a continuous distribution from the two-photon decay of the $2\,^1S_0$ state.

This results in the observed high selectivity during the K-shell ionization of the Li-like ions populating exclusively the excited $2\,^1S_0$ and the $2\,^3S_1$ states of He-like uranium. This finding has already been explored in detail and utilized in recent studies

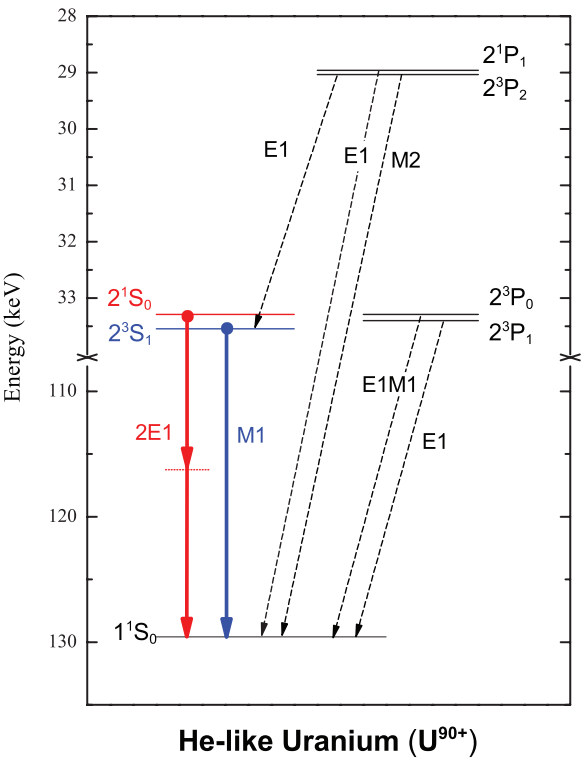

FIG. 3. (Color online) Decay scheme of He-like uranium. Of particular importance for this measurement are: the $M1$ ($2\,^3S_1 \rightarrow 1\,^1S_0$) magnetic dipole and the $2E1$ ($2\,^1S_0 \rightarrow 1\,^1S_0$) - two-photon transitions.

performed by our group for Li-like tin [26] and uranium [30] ions, in which also the origin of this high state selectivity was discussed in detail. This new technique for the selective population of the $2\,^1S_0$ and $2\,^3S_1$ excited states in He-like ions provides unique access to an almost background-free two-photon spectral distribution. In particular, because the $2s$ electron stays passive during the collision, the measured $M1$ line and especially the $2E1$ energy distribution are not distorted by $E1$ and $E1M1$ decays from the $2\,^3P_1$ and the $2\,^3P_0$ states, respectively.

IV. SPECTRA ANALYSIS

In order to compare the observed two-photon spectra with theoretical predictions, the influence of the detector response function has to be taken into account. Knowledge of this response function is important for the precise measurement of the two-photon energy distribution especially in the high-energy regime where the Compton scattering in the detector becomes non-negligible. In this case, the $M1$ photons can be detected as low-energy photons and can thus modify the shape of the two-photon energy distribution. The germanium detector response function was simulated with a well-established Monte Carlo EGS4 code system [33] including the LSCAT (low-energy photon-scattering expansion) package [34]. In the simulation, the photoelectric effect, Compton effect for bound electrons, and Rayleigh scattering, as well as L- and K-shell fluorescence were considered. The geometrical model included a point source (gas-target beam), two beryllium windows (ESR beamline port and the detector entrance), and a cylindrical germanium crystal (sensitive volume of the detector). The dimensions and distances were chosen according to the experimental setup. The simulation results were convoluted with the energy-dependent resolution of the detector and a correction for the Doppler broadening due to the finite opening angle of the detector. The resolution as a function of energy was obtained by calibration using the monoenergetic lines from the radioactive sources of ^{57}Co, ^{133}Ba, ^{152}Eu, ^{207}Bi, and ^{241}Am. For the particular detector (mounted at the 35° observation angle), the obtained energy resolution amounted to 390 and 520 eV for 60 and 120 keV, respectively. The Doppler broadening was calculated using the following formula:

$$\Delta E_\gamma^{\mathrm{lab}} = E_\gamma^{\mathrm{lab}} \frac{\beta \sin\theta}{1-\beta\cos\theta}\Delta\theta, \tag{1}$$

where E_γ^{lab} is the photon energy in the laboratory frame which is related to the photon energy in the emitter (ion) frame by the relativistic Doppler transformation:

$$E_\gamma^{\mathrm{lab}} = \frac{E_\gamma^{\mathrm{em}}}{\gamma}\frac{1}{1-\beta\cos\theta}. \tag{2}$$

Here, β and γ are the relativistic factors corresponding to the particular ion beam energy and θ is the observation angle in the laboratory frame. $\Delta\theta$ is the detector opening angle (the uncertainty of the observation angle). It was calculated according to the following detector-chamber geometry: the detector to reaction-area distance of 390 mm for the particular detector position with respect to the ion beam direction (at the 35° observation angle) and the detector slit width of 6 mm. This results in $\Delta\theta$ of the order of 1° leading to the Doppler broadening of about ∼1 and 2 keV for the photon energies of 60 and 120 keV, respectively. As a consequence, the linewidth used in the simulation is mainly determined by the Doppler broadening.

V. RESULTS AND DISCUSSION

In Fig. 4, the $2E1$ two-photon distribution measured by the detector placed at 35°, corrected for the detector efficiency and absorption in the chamber window, is compared with our relativistic calculations [29]. For comparison, the theoretical two-photon spectral shape and the detector response function for the $M1$ transition, both convoluted with the detector resolution and the Doppler broadening (as explained in Sec. IV), plus a linear background were fitted to the experimental spectrum. The result of this fit procedure is depicted in the figure by the black dashed curve. In addition, we show separately both parts obtained from the fit; the detector response function for the $M1$ transition convoluted with the detector resolution and the Doppler broadening (blue dotted curve), and the theoretical two-photon spectral shape convoluted with the detector resolution and the Doppler broadening plus background (red solid curve). The comparison shows good agreement between the theoretical two-photon distribution (convoluted with the detector response function) and the experimental spectrum. Only small discrepancies are observed in the region close to the $M1$ line. These are most likely the result of a low-energy asymmetry of the $M1$ line that arises from artifacts of the detector, such as the incomplete charge collection, which are not included in the simulation. Generally, Fig. 4 shows that the correction for the $M1$ line

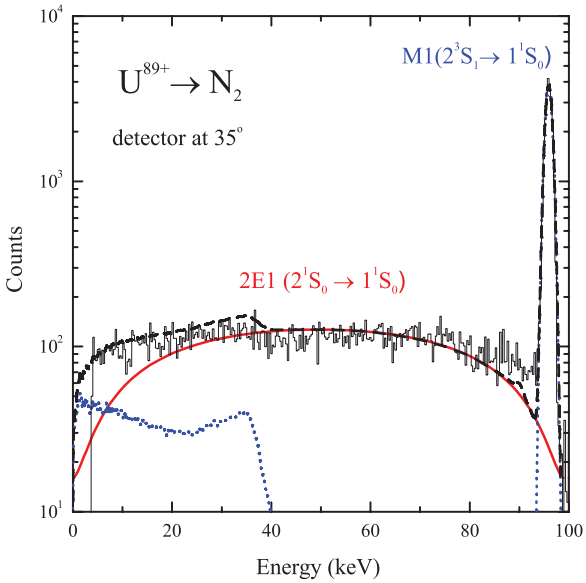

FIG. 4. (Color online) X-ray spectrum registered at 35° in coincidence with ionization of Li-like uranium ions (solid black line) in comparison with our relativistic calculations. The theoretical two-photon spectral shape (solid red curve) and the detector response function for the $M1$ transition (dotted blue curve), both convoluted with the detector resolution and the Doppler broadening, plus a linear background were fitted to the experimental spectrum. The result of this fit procedure is shown by the black dashed curve.

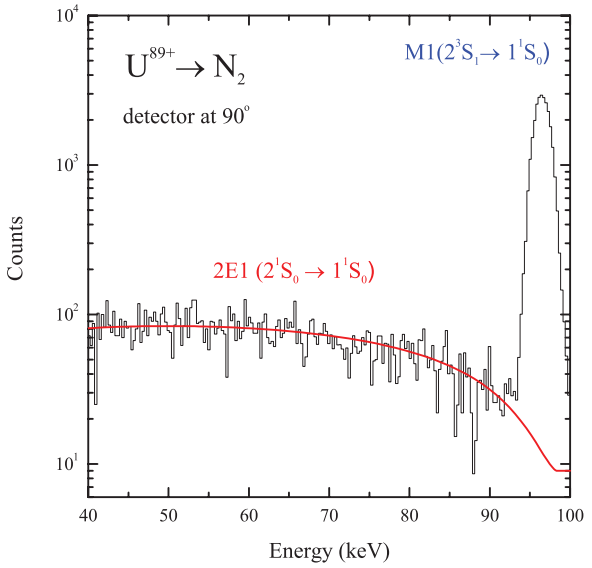

FIG. 5. (Color online) X-ray spectrum registered at 90° in coincidence with the ionization of Li-like uranium ions (solid black line). The theoretical two-photon spectral shape convoluted with the detector resolution and the Doppler broadening plus a linear background is fitted to the experimental spectrum (red solid curve).

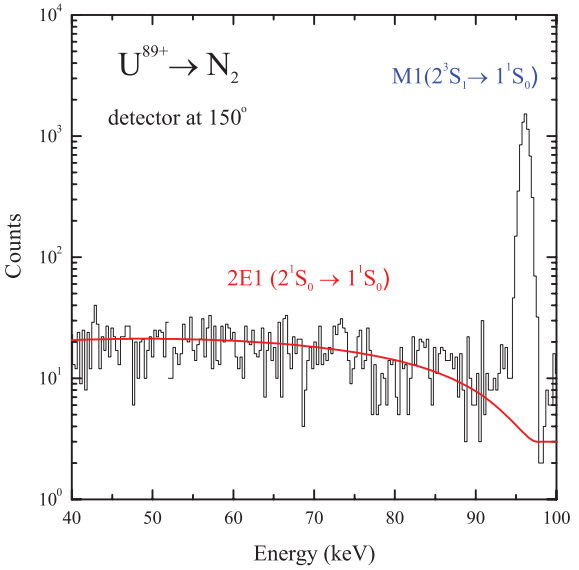

FIG. 6. (Color online) X-ray spectrum registered at 150° in coincidence with the ionization of Li-like uranium ions (solid black line). The theoretical two-photon spectral shape convoluted with the detector resolution and the Doppler broadening plus a linear background is fitted to the experimental spectrum (red solid curve).

response function is only important for the left (low-energy) branch of the measured $2E1$ energy distribution. We also checked that the inclusion of the detector response function for the $M1$ line does not significantly affect the final fit results (the comparison between the experiment and theory) quantitatively, for the right (high-energy) branch of the spectrum. Since the low-energy branch is also very sensitive to absorption in the chamber windows and to the detector efficiency corrections for low x-ray energies, in our further analysis only the right part of the distribution was considered. This method of the data analysis is possible thanks to the symmetry of the $2E1$ spectral shape with respect to the half of the transition energy fraction [28,29].

In Figs. 5 and 6, the two-photon energy distributions measured at 90° and 150° observation angles are compared with our relativistic calculations. The comparison is done in the same way as for the case of the detector at 35°, but excluding the detector response function for the $M1$ transition (see above). Again, good agreement is found between the experimental data and the calculated spectral distribution.

Furthermore, from the measured distribution, a reduced FWHM was obtained. For this, the $M1$ peak was subtracted from the spectra and the right branch of the experimental distribution was fitted with a polynomial function. The reduced FWHM was calculated as a ratio of the width of the right part of the distribution multiplied by 2 and the maximum possible photon energy (as given by the $2\,{}^1S_0 \rightarrow 1\,{}^1S_0$ transition energy). We obtained the following values for the reduced FWHM of the spectral distributions measured at different angles: $\sim 0°$, 0.81 ± 0.069; 35°, 0.76 ± 0.052; 90°, 0.64 ± 0.055; 120°, 0.73 ± 0.046; 150°, 0.72 ± 0.047, resulting in a mean value of 0.73 ± 0.028. In Fig. 7, our experimental result is compared with the theoretical values for the reduced FWHM. In addition, the experimental result obtained by Schäffer *et al.* [23] for Ni^{26+} ions is shown. The comparison of our experimental result with theory shows a clear deviation from the nonrelativistic prediction and very good agreement with the relativistic calculations including the QED treatment of the electron-electron interaction used in [29]. This unambiguously confirms the importance of the relativistic effects for the $2E1$ two-photon decay energy distribution. Here, we like to add that the relativistic values for FWHM obtained by Derevianko

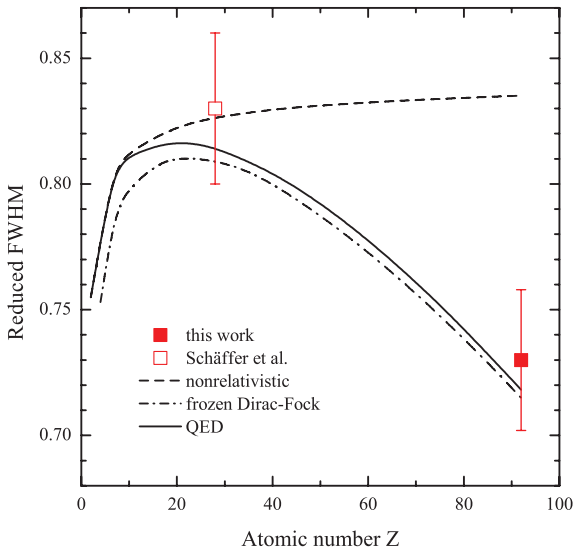

FIG. 7. (Color online) Comparison of the measured reduced FWHM of the $2E1$ two-photon distribution (red solid square) with the nonrelativistic (dashed curve) and relativistic predictions based on the frozen Dirac-Fock method (dash-dotted curve) and QED treatment of electron-electron interaction (solid line). The nonrelativistic and relativistic theoretical values for $Z \leqslant 10$ were taken from [35] and [28], respectively. The result for Ni^{26+} ions was added based on Schäffer *et al.* [23] (red open square).

and Johnson [28] were found to be in good agreement with the results of our relativistic calculations [29]. The current experimental result for He-like uranium cannot distinguish between the relativistic prediction which takes into account the electron-electron interaction rigorously up to the first order in the QED perturbation expansion [29] and the value obtained within the frozen Dirac-Fock method which implements an independent-particle model in which single-electron orbitals are of the Dirac-Fock type. Further experimental studies would be desirable to distinguish between these two calculations and thus gain more insight into the electronic correlations in the presence of strong Coulomb fields.

VI. SUMMARY

We performed a measurement of the $2E1$ two-photon energy distribution from the decay of the $1s2s\ ^1S_0$ level in He-like uranium. For this purpose, a recently developed technique of virtually background-free two-photon transition measurements was used. In this measurement, the excited He-like uranium ions are formed by a K-shell ionization of initially Li-like species in collisions with a light target and the x rays from the decay of the excited He-like ions are measured. The observed intense production of the $2E1$ transitions and a very high level selectivity makes this process particularly well suited for studying of the two-photon spectral shape and thus for a detailed investigation of the structure of high-Z He-like systems. Note, that the very short lifetimes of the levels in heavy ions make standard lifetime measurements practically impossible.

The measured shape of the $2E1$ two-photon energy distribution in the He-like uranium agrees well with the results of our relativistic calculations which take into account the electron-electron interaction rigorously up to the first order in the QED perturbation expansion. Moreover, the FWHM extracted from the measured two-photon distribution unequivocally favors the relativistic predictions over the nonrelativistic results and thus confirms the predicted narrowing of the shape in the high-Z domain due to the relativistic effects. Our current and recent [26] studies have proven the potential of the spectral distribution analysis for a better understanding of the relativistic effects in the two-photon processes. A further increase of the statistical accuracy as well as experimental improvements such as the two-photon angular and polarization correlation measurements will enable us to further deepen insights into electron-electron correlation phenomena in the strong-field regime.

ACKNOWLEDGMENTS

This work was supported by the Polish Ministry of Science and Higher Education under Grant No. N N202 463539 and the Helmholtz Alliance Program of the Helmholtz Association, Contract No. HA216/EMMI "Extremes of Density and Temperature: Cosmic Matter in the Laboratory." A.S. acknowledges support from the Helmholtz Gemeinschaft and GSI under project No. VH-NG-421. X.M. is supported by the External Cooperation Program of the Chinese Academy Sciences, Grant No. GJHZ1305. We would like to express our thanks to the members of the ESR team for their collaboration.

[1] M. Göppert-Mayer, Ann. Physik. **90**, 273 (1931).
[2] G. Breit and E. Teller, Astrophys. J. **91**, 215 (1940).
[3] P. H. Mokler and R. W. Dunford, Phys. Scr. **69**, C1 (2004).
[4] A. S. Pearl, Phys. Rev. Lett. **24**, 703 (1970).
[5] R. S. Van Dyck, Jr., C. E. Johnson, and H. A. Shugart, Phys. Rev. A **4**, 1327 (1971).
[6] M. H. Prior and H. A. Shugart, Phys. Rev. Lett. **27**, 902 (1971).
[7] R. Marrus and R. W. Schmieder, Phys. Rev. A **5**, 1160 (1972).
[8] R. W. Dunford, H. G. Berry, K. O. Groeneveld, M. Hass, E. Bakke, M. L. A. Raphaelian, A. E. Livingston, and L. J. Curtis, Phys. Rev. A **38**, 5423 (1988).
[9] R. W. Dunford, M. Hass, E. Bakke, H. G. Berry, C. J. Liu, M. L. A. Raphaelian, and L. J. Curtis, Phys. Rev. Lett. **62**, 2809 (1989).
[10] R. W. Dunford, H. G. Berry, D. A. Church, M. Hass, C. J. Liu, M. L. A. Raphaelian, B. J. Zabransky, L. J. Curtis, and A. E. Livingston, Phys. Rev. A **48**, 2729 (1993).
[11] R. W. Dunford, D. A. Church, C. J. Liu, H. G. Berry, M. L. A. Raphaelian, M. Hass, and L. J. Curtis, Phys. Rev. A **41**, 4109 (1990).
[12] R. W. Dunford, H. G. Berry, S. Cheng, E. P. Kanter, C. Kurtz, B. J. Zabransky, A. E. Livingston, and L. J. Curtis, Phys. Rev. A **48**, 1929 (1993).
[13] R. Marrus, V. San Vicente, P. Charles, J. P. Briand, F. Bosch, D. Liesen, and I. Varga, Phys. Rev. Lett. **56**, 1683 (1986).
[14] R. Marrus, P. Charles, P. Indelicato, L. de Billy, C. Tazi, J.-P. Briand, A. Simionovici, D. D. Dietrich, F. Bosch, and D. Liesen, Phys. Rev. A **39**, 3725 (1989).
[15] A. Simionovici, B. B. Birkett, J.-P. Briand, P. Charles, D. D. Dietrich, K. Finlayson, P. Indelicato, D. Liesen, and R. Marrus, Phys. Rev. A **48**, 1695 (1993).
[16] S. Toleikis, B. Manil, E. Berdermann, H. F. Beyer, F. Bosch, M. Czanta, R. W. Dunford, A. Gumberidze, P. Indelicato, C. Kozhuharov *et al.*, Phys. Rev. A **69**, 022507 (2004).
[17] C. T. Munger and H. Gould, Phys. Rev. Lett. **57**, 2927 (1986).
[18] M. Lipeles, R. Novick, and N. Tolk, Phys. Rev. Lett. **15**, 690 (1965).
[19] R. C. Elton, L. J. Palumbo, and H. R. Griem, Phys. Rev. Lett. **20**, 783 (1968).
[20] D. O'Connell, K. J. Kollath, A. J. Duncan, and H. Kleinpoppen, J. Phys. B **8**, L214 (1975).
[21] R. Ali, I. Ahmad, H. G. Berry, R. W. Dunford, D. S. Gemmell, E. P. Kanter, P. H. Mokler, A. E. Livingston, S. Cheng, and L. J. Curtis, Nucl. Instrum. Methods Phys. Res., Sect. B **98**, 69 (1995).
[22] R. Ali, I. Ahmad, R. W. Dunford, D. S. Gemmell, M. Jung, E. P. Kanter, P. H. Mokler, H. G. Berry, A. E. Livingston, S. Cheng *et al.*, Phys. Rev. A **55**, 994 (1997).

[23] H. W. Schäffer, P. H. Mokler, R. W. Dunford, C. Kozhuharov, A. Krämer, T. Ludziejewski, H.-T. Prinz, P. Rymuza, L. Sarkadi, T. Stöhlker *et al.*, Phys. Scr. **T80**, 469 (1999).
[24] R. W. Dunford, E. P. Kanter, H. W. Schäffer, P. H. Mokler, H. G. Berry, A. E. Livingston, S. Cheng, and L. J. Curtis, Phys. Scr. **T80**, 143 (1999).
[25] H. W. Schäffer, R. W. Dunford, E. P. Kanter, S. Cheng, L. J. Curtis, A. E. Livingston, and P. H. Mokler, Phys. Rev. A **59**, 245 (1999).
[26] S. Trotsenko, A. Kumar, A. V. Volotka, D. Banaś, H. F. Beyer, H. Bräuning, S. Fritzsche, A. Gumberidze, S. Hagmann, S. Hess *et al.*, Phys. Rev. Lett. **104**, 033001 (2010).
[27] G. W. F. Drake, Phys. Rev. A **34**, 2871 (1986).
[28] A. Derevianko and W. R. Johnson, Phys. Rev. A **56**, 1288 (1997).
[29] A. V. Volotka, A. Surzhykov, V. M. Shabaev, and G. Plunien, Phys. Rev. A **83**, 062508 (2011).
[30] J. Rzadkiewicz, Th. Stöhlker, D. Banaś, H. F. Beyer, F. Bosch, C. Brandau, C. Z. Dong, S. Fritzsche, A. Gojska, A. Gumberidze *et al.*, Phys. Rev. A **74**, 012511 (2006).
[31] C. Scheidenberger, T. Stöhlker, W. E. Meyerhof, H. Geissel, P. H. Mokler, and B. Blank, Nucl. Instrum. Methods Phys. Res., Sect. B **142**, 441 (1998).
[32] M. Pajek, A. P. Kobzev, R. Sandrik, R. A. Ilkhamov, and S. H. Khusmurodov, Nucl. Instrum. Methods Phys. Res., Sect. B B **42**, 346 (1989).
[33] W. R. Nelson, H. Hirayama, and D. W. O. Rogers, Stanford Linear Accelerator Center report SLAC-265 (1985).
[34] Y. Namito and H. Hirayama, KEK Internal 2000-4, May (2000).
[35] G. W. F. Drake, G. A. Victor, and A. Dalgarno, Phys. Rev. **180**, 25 (1969).